Université de Mons
Faculté Polytechnique – Service de Mécanique Rationnelle, Dynamique et Vibrations
31, Bld Dolez - B-7000 MONS (Belgique)
065/37 42 15 – georges.kouroussis@umons.ac.be

B. Olivier, O. Verlinden, G. Kouroussis, Stability and error analysis of applied-force co-simulation methods using mixed one-step integration schemes, In B. Schweizer (ed.), *IUTAM Symposium on Solver-Coupling and Co-Simulation*, Chapter 12, pp. 243–254, ISBN 978-3-030-14883-6, 2019.

Chapter 12
Stability and Error Analysis of Applied-Force Co-simulation Methods Using Mixed One-Step Integration Schemes

Bryan Olivier, Olivier Verlinden and Georges Kouroussis

Abstract Co-simulation schemes are designed to couple subsystems during the integration process. Therefore, any complex or multi-physics system can be split into subsystems in its mathematical representation, and re-coupled using a co-simulation scheme. Dealing separately with each subsystem, its own characteristics and specifically its own solver is the purpose of this decoupling/re-coupling mechanism. Before making a choice between all the existing solver-coupling schemes for a complex mechanical system, it is interesting to know which one is the most efficient. Therefore, this paper studies the performance of the Jacobi and Gauß–Seidel methods using one-step integration schemes applied on a double harmonic oscillator. However, since most of the mechanical joints generate elastic forces, the study concerns applied-force schemes only.

12.1 Introduction

To couple two (or more) dynamic models, it is often better to consider each model in the appropriate approach, to avoid a single and rigorous analysis and to prefer a decoupled approach. For example, in order to predict ground vibrations induced by railway vehicles, it is common to develop decoupled vehicle/track/soil models [1–3]. The model proposed by Kouroussis et al. [4] is a sequential two-step model that uses a multibody modeling approach for the vehicle/track subsystem (including

B. Olivier (✉) · O. Verlinden · G. Kouroussis
Faculty of Engineering, Department of Theoretical Mechanics,
Dynamics and Vibrations, University of Mons, Place du Parc 20, 7000 Mons, Belgium
e-mail: bryan.olivier@umons.ac.be

O. Verlinden
e-mail: olivier.verlinden@umons.ac.be

G. Kouroussis
e-mail: georges.kouroussis@umons.ac.be

B. Schweizer (ed.), *IUTAM Symposium on Solver-Coupling and Co-Simulation*,
IUTAM Bookseries 35, https://doi.org/10.1007/978-3-030-14883-6_12

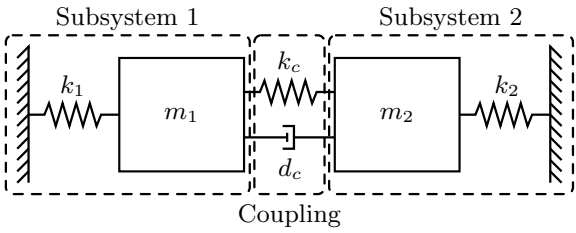

Fig. 12.1 Double Harmonic Oscillator with masses m_i, stiffnesses k_i and damping coefficient d_c

also a reduced model of the soil) for the first step and, for the second step, a finite element model for the soil to simulate ground vibration propagation. This two-step simulation process using different solvers could be transformed into a co-simulation process. Therefore, it is important to determine where the global model (vehicle-rails-sleepers-ballast-soil) must be split and which co-simulation scheme provides the best results. Since each section where the system could be split generates elastic constraints, only applied-forces co-simulation schemes will be considered.

This study presents an error analysis and also investigates the numerical stability of two co-simulation schemes: the Jacobi and Gauß–Seidel schemes [5] applied to a double harmonic oscillator with different stiffness ratios (Fig. 12.1). Research in this field was already performed by Busch [5], however, this paper proposes an alternative way to build the amplification matrices [6] of co-simulated mechanical subsystems with their respective integration scheme. Furthermore, the impact of the solver used for each subsystem and the coupling effect of two different solvers are also investigated.

Figure 12.1 represents the system studied in this paper. Separated, the subsystems i (composed of a mass m_i and connected to the reference body with a spring of stiffness k_i where $i = 1, 2$) are supposed to be undamped in order to distinguish the numerical damping caused by both numerical integration and coupling schemes. The coupling joint (represented by k_c and d_c), however, presents damping to limit instabilities. Since the link between subsystem 1 and subsystem 2 is flexible, both systems are re-coupled by forces. The choice of applied-force coupling schemes has two main interests:

– Any native elastic joint (even with damping) can be used to split an entire system.
– Rigid joints can be approximated by increasing the stiffness of the link (k_c) in the model (when $k_c \to \infty$, a situation close to the gluing is created but since the value of the stiffness has to be defined, the method does not include algebraic constraints).

Furthermore, different stiffness ratios are studied to illustrate the performance of Jacobi and Gauß–Seidel co-simulation schemes in different situations representing different physical phenomena.

12.2 Amplification Matrix Construction

The amplification matrix that defines the modification of the state variables over a time step has interesting properties that qualify the numerical schemes used to integrate a given system. Before analyzing its properties, the following lines describe how to construct that matrix. The method described here is comparable with the method proposed by Busch [5].

Considered separately, each subsystem i consists of a harmonic oscillator with its own eigenfrequency $\omega_{0i} = \sqrt{\frac{k_i}{m_i}}$. Therefore, the equation of motion of this system is

$$\ddot{y}_i + \omega_{0i}^2 y_i = 0 \tag{12.1}$$

which is equivalent, for first integration schemes, to

$$\begin{bmatrix} 1 & 0 \\ 0 & 1 \end{bmatrix} \dot{\mathbf{x}}_i + \begin{bmatrix} 0 & -1 \\ \omega_{0i}^2 & 0 \end{bmatrix} \mathbf{x}_i = 0 \quad \text{if} \quad \mathbf{x}_i = \begin{Bmatrix} y_i \\ \dot{y}_i \end{Bmatrix}. \tag{12.2}$$

Considering a one-step and first-order numerical integration formula $\boldsymbol{\Lambda}$, the discretized system becomes

$$\begin{bmatrix} 1 & 0 \\ 0 & 1 \end{bmatrix} \dot{\mathbf{x}}_i^{t+h} + \begin{bmatrix} 0 & -1 \\ \omega_{0i}^2 & 0 \end{bmatrix} \mathbf{x}_i^{t+h} = 0 \tag{12.3a}$$

$$\boldsymbol{\Lambda}(\mathbf{x}_i^t, \dot{\mathbf{x}}_i^t, \mathbf{x}_i^{t+h}, \dot{\mathbf{x}}_i^{t+h}) = 0 \tag{12.3b}$$

and can be re-written in the form

$$\mathbf{P}_i \mathbf{z}_i^{t+h} + \mathbf{Q}_i \mathbf{z}_i^t = 0 \tag{12.4}$$

where $\mathbf{z}_i^{t+h} = \left\{ \mathbf{x}_i^{t+h} \; \dot{\mathbf{x}}_i^{t+h} \right\}^{\mathrm{T}}$ and $\mathbf{z}_i^t = \left\{ \mathbf{x}_i^t \; \dot{\mathbf{x}}_i^t \right\}^{\mathrm{T}}$.

It can be noticed that Eq. 12.4 can be written for any mechanical system with n_{cp} configuration parameters and leads to $4n_{cp}$ equations (for mechanical systems described by a first order formulation). Furthermore, it yields the discretized state space representation

$$\mathbf{z}_i^{t+h} = -\mathbf{P}_i^{-1} \mathbf{Q}_i \mathbf{z}_i^t = \mathbf{A}_i^0 \mathbf{z}_i^t \tag{12.5}$$

where $\mathbf{A}_i^0$ is the amplification matrix of the uncoupled subsystem i.

12.2.1 Amplification Matrix of Co-simulation Schemes

As for classical integration schemes, the evolution of the state variables (configuration parameters and their first time derivative for mechanical systems) over a time step can be expressed, for a given co-simulation scheme, as:

$$\mathbf{z}^{t+h} = \mathbf{A}^{CS}\mathbf{z}^{t} \tag{12.6}$$

representing the relationship between the state variables at time t and $t+h$ due to the integration scheme. The coupling amplification matrix $\mathbf{A}^{CS}$ is a function of the time step, both subsystems, the integration schemes used and, furthermore, the coupling scheme used. For both subsystems, the discretized state space representation becomes, to take the coupling into account,

$$\mathbf{P}_i\mathbf{z}_i^{t+h} + \mathbf{Q}_i\mathbf{z}_i^{t} + \mathbf{R}_i\mathbf{u}_i = 0 \tag{12.7}$$

in which:

- $\mathbf{R}_i$ matrix has a size of $4n_{cp} \times n_{cv}$ and defines how the subsystems are interacting (with n_{cv}, the number of coupling variables). This matrix could also be used in the monolithic system (in opposition to the co-simulated system) in order to define the interaction between both equations of the entire system.
- $\mathbf{u}_i$ vector has a length of $n_{cv} \times 1$ and defines the coupling variables chosen, for each subsystem, with respect to the state variables of the others. This vector defines the coupling scheme used to perform the integration.

In general, for both subsystems, the inputs are developed in,

$$\mathbf{u}_i = \mathbf{U}_i^{t}\mathbf{z}_{j\neq i}^{t} + \mathbf{U}_i^{t+h}\mathbf{z}_{j\neq i}^{t+h} \tag{12.8}$$

where $\mathbf{U}_i^t$ and $\mathbf{U}_i^{t+h}$ defines the connexion scheme between both subsystems and, among other things, the order in which both subsystems are integrated and how the coupling variables are predicted for the second integration when the scheme is sequential. In particular, in our system without any link damping ($d_c = 0 \rightarrow n_{cv} = 1$), taking into account that $\mathbf{z}_1^t = \left\{y_1^t\ \dot{y}_1^t\ \dot{y}_1^t\ \ddot{y}_1^t\right\}^{\mathrm{T}}$ and $\mathbf{z}_2^t = \left\{y_2^t\ \dot{y}_2^t\ \dot{y}_2^t\ \ddot{y}_2^t\right\}^{\mathrm{T}}$ ($\dot{y}_1^t$ and $\dot{y}_2^t$ are taken twice into account due to the first order transformation of the second order equations of motion), the following cases can happen:

- $\mathbf{U}_1^t = [\,1\,0\,0\,0\,]$, $\mathbf{U}_1^{t+h} = [\,0\,0\,0\,0\,]$, $\mathbf{U}_2^t = [\,1\,0\,0\,0\,]$ and $\mathbf{U}_2^{t+h} = [\,0\,0\,0\,0\,]$ correspond to the Jacobi scheme (illustrated in Fig. 12.2b) in which each integration does not influence each other over the same macro-time step.
- $\mathbf{U}_1^t = [\,1\,0\,0\,0\,]$, $\mathbf{U}_1^{t+h} = [\,0\,0\,0\,0\,]$, $\mathbf{U}_2^t = [\,0\,0\,0\,0\,]$ and $\mathbf{U}_2^{t+h} = [\,1\,0\,0\,0\,]$ correspond to the Gauß–Seidel scheme (illustrated in Fig. 12.2a) where the first subsystem is integrated without any interaction with subsystem 2 (such as in Jacobi scheme) but the second subsystem is integrated using the output of the first integration. This scheme is completely sequential.
- $\mathbf{U}_1^t = [\,0\,0\,0\,0\,]$, $\mathbf{U}_1^{t+h} = [\,1\,0\,0\,0\,]$, $\mathbf{U}_2^t = [\,1\,0\,0\,0\,]$ and $\mathbf{U}_2^{t+h} = [\,0\,0\,0\,0\,]$ lead to the same as the previous scheme but in which subsystem 2 is integrated before subsystem 1.
- $\mathbf{U}_1^t = [\,0\,0\,0\,0\,]$, $\mathbf{U}_1^{t+h} = [\,1\,0\,0\,0\,]$, $\mathbf{U}_2^t = [\,0\,0\,0\,0\,]$ and $\mathbf{U}_2^{t+h} = [\,1\,0\,0\,0\,]$ correspond to a scheme where each subsystem is integrated before the other one which is practically impossible. Using Eqs. 12.7 and 12.8 with that schemes yields the amplification matrix of the monolithic system. However, even if it is possible with

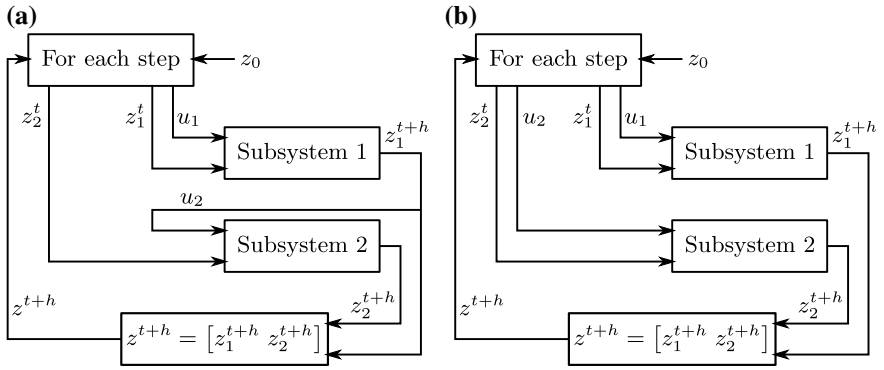

Fig. 12.2 Gauß–Seidel (2a) and Jacobi (2b) co-simulation schemes: step procedure with initial conditions z_0, subsystem i state variables z_i and subsystem i inputs u_i

that simple example, iteration becomes necessary when working with dedicated software packages for each subsystem.

To obtain those matrices for the system with a link damping ($d_c \neq 0 \rightarrow n_{cv} = 2$), a second line must be added with a 1 in the third column (or second due to the transformation of second order mechanical equations in first order equations) to select the speed as a second coupling variable.

For two subsystems, Eqs. 12.7 and 12.8 become

$$\mathbf{z}_1^{t+h} + \mathbf{P}_1^{-1}\mathbf{Q}_1\mathbf{z}_1^t + \mathbf{P}_1^{-1}\mathbf{R}_1\left(\mathbf{U}_1^t\mathbf{z}_2^t + \mathbf{U}_1^{t+h}\mathbf{z}_2^{t+h}\right) = 0 \tag{12.9a}$$

$$\mathbf{z}_2^{t+h} + \mathbf{P}_2^{-1}\mathbf{Q}_2\mathbf{z}_2^t + \mathbf{P}_2^{-1}\mathbf{R}_2\left(\mathbf{U}_2^t\mathbf{z}_1^t + \mathbf{U}_2^{t+h}\mathbf{z}_1^{t+h}\right) = 0 \tag{12.9b}$$

in which $\mathbf{P}_2^{-1}\mathbf{Q}_2$ and $\mathbf{P}_2^{-1}\mathbf{Q}_2$ are, using Eq. 12.5, the opposite of the amplification matrices $-\mathbf{A}_1^0$ and $-\mathbf{A}_2^0$ of each uncoupled subsystem. This system yields the matrix form

$$\begin{bmatrix} \mathbf{I} & \mathbf{P}_1^{-1}\mathbf{R}_1\mathbf{U}_1^{t+h} \\ \mathbf{P}_2^{-1}\mathbf{R}_2\mathbf{U}_2^{t+h} & \mathbf{I} \end{bmatrix} \begin{Bmatrix} \mathbf{z}_1^{t+h} \\ \mathbf{z}_2^{t+h} \end{Bmatrix} + \begin{bmatrix} -\mathbf{A}_1^0 & \mathbf{P}_1^{-1}\mathbf{R}_1\mathbf{U}_1^t \\ \mathbf{P}_2^{-1}\mathbf{R}_2\mathbf{U}_2^t & -\mathbf{A}_2^0 \end{bmatrix} \begin{Bmatrix} \mathbf{z}_1^t \\ \mathbf{z}_2^t \end{Bmatrix} = 0 \tag{12.10}$$

that could be shortened in the generic form

$$\mathbf{P}^{CS}\mathbf{z}^{t+h} + \mathbf{Q}^{CS}\mathbf{z}^t = 0 \tag{12.11}$$

if $\mathbf{z}^{t,t+h} = \left\{\mathbf{z}_1^{t,t+h}\ \mathbf{z}_2^{t,t+h}\right\}^{\mathrm{T}}$. Finally, such as for classical monolithic systems, the amplification matrix of co-simulation methods is expressed by

$$\mathbf{A}^{CS} = -\left(\mathbf{P}^{CS}\right)^{-1}\mathbf{Q}^{CS} \tag{12.12}$$

where $\mathbf{P}^{CS}$ and $\mathbf{Q}^{CS}$ are defined by Eqs. 12.10 and 12.11 where $\mathbf{I}$ is the identity matrix with a size tuned to the number of variables $\mathbf{z}_i$ of subsystem i scheme.

A few remarks can be made on Eq. 12.10:

- The coupling between both subsystems clearly appears through the non-diagonal terms. Indeed, if both $\mathbf{R}_i$ are matrices filled with zeros, both systems appear to be fully decoupled and the amplification matrix contains only both uncoupled amplification matrices $\mathbf{A}_1^0$ and $\mathbf{A}_2^0$.
- When $\mathbf{U}_i^{t+h}$ is filled with zeros, the corresponding subsystem is not explicitly dependent upon the second subsystem integrated states variables.
- When both $\mathbf{U}_i^t$ are filled with zeros, the amplification matrix obtained corresponds to the monolithic system matrix. As specified earlier, this scheme is practically unreachable with a co-simulation scheme without infinite iterations.

12.2.2 Amplification Matrix of Iterated Schemes

When the accuracy of the solution is more important than the computation time, the co-simulation scheme can be iterated in order to improve accuracy and numerical stability. Indeed, in Eq. 12.7, the closer $\mathbf{u}_i$ and $\mathbf{z}_{j\neq j}^{t+h}$, the closer the co-simulation and the monolithic schemes should be. Hence, for a given coupling scheme, a first integration of both subsystems could be performed to have a better estimation of $\mathbf{u}_i$ values in a second full integration.

Taking into account iterations in the co-simulation scheme, the state space representation of a subsystem scheme, Eq. 12.7 becomes, for the kth iteration of a given scheme:

$$\mathbf{P}_i \mathbf{z}_i^{t+h,k} + \mathbf{Q}_i \mathbf{z}_i^t + \mathbf{R}_i \mathbf{u}_i^k = 0 \tag{12.13}$$

where $\mathbf{z}_i^{t+h,k}$ is the kth iteration of the state variables and $\mathbf{u}_i^k$ is the kth iteration of the inputs of subsystem i. These inputs are obtained by modifying adequately Eq. 12.8:

$$\mathbf{u}_i^k = \mathbf{U}_i^{s,k} \mathbf{z}_{j\neq i}^{t+h,k} + \mathbf{U}_i^{s-1,k} \mathbf{z}_{j\neq i}^{t+h,k-1} \tag{12.14}$$

where, such as for non-iterated systems, the matrices $\mathbf{U}_i^{s,k}$ and $\mathbf{U}_i^{s-1,k}$ define the procedure followed to integrate both subsystems during the iteration process. Indeed, if k represents the number of iterations, $\mathbf{U}_i^{s,k}$ defines whether the integration of subsystem i is takes into account an estimation of the state variables $\mathbf{z}_{j\neq i}^{t+h,k}$ resulting from an integration of the other subsystem during the same kth iteration. However, $\mathbf{U}_i^{s,k}$ defines whether the integration of subsystem i takes into account the estimation of the state variables $\mathbf{z}_{j\neq i}^{t+h,k-1}$ resulting from the previous iteration $k-1$th. It must be remarked that an extrapolation of the state variables obtained in N previous iterations could lead to a faster convergence to the monolithic scheme. In this study, the iteration matrices are defined as follows (for the undamped coupling scheme):

- $\mathbf{U}_1^{s,k} = [\,0\,0\,0\,0\,]$, $\mathbf{U}_1^{s,k-1} = [\,1\,0\,0\,0\,]$, $\mathbf{U}_2^{s,k} = [\,0\,0\,0\,0\,]$ and $\mathbf{U}_2^{s,k-1} = [\,1\,0\,0\,0\,]$ which leads to a iterated-Jacobi scheme or

– $\mathbf{U}_1^{s,k} = [0\,0\,0\,0]$, $\mathbf{U}_1^{s,k-1} = [1\,0\,0\,0]$, $\mathbf{U}_2^{s,k} = [1\,0\,0\,0]$ and $\mathbf{U}_2^{s,k-1} = [0\,0\,0\,0]$ which leads to a iterated-Gauß-Seidel scheme;
– these matrices could vary between two successive iterations.

Considering Eqs. 12.13 and 12.14, for two subsystems solved by an iterated co-simulation scheme, it can be written

$$\mathbf{P}_1\mathbf{z}_1^{t+h,k} + \mathbf{Q}_1\mathbf{z}_1^{t} + \mathbf{R}_1\left(\mathbf{U}_1^{s,k}\mathbf{z}_2^{t+h,k} + \mathbf{U}_1^{s-1,k}\mathbf{z}_2^{t+h,k-1}\right) = 0 \tag{12.15a}$$

$$\mathbf{P}_2\mathbf{z}_2^{t+h,k} + \mathbf{Q}_2\mathbf{z}_2^{t} + \mathbf{R}_2\left(\mathbf{U}_2^{s,k}\mathbf{z}_1^{t+h,k} + \mathbf{U}_2^{s-1,k}\mathbf{z}_1^{t+h,k-1}\right) = 0 \tag{12.15b}$$

which can be expressed in the following matrix form

$$\begin{bmatrix} \mathbf{P}_1 & \mathbf{R}_1\mathbf{U}_1^{s,k} \\ \mathbf{R}_2\mathbf{U}_2^{s,k} & \mathbf{P}_2 \end{bmatrix} \begin{Bmatrix} \mathbf{z}_1^{t+h,k} \\ \mathbf{z}_2^{t+h,k} \end{Bmatrix} + \begin{bmatrix} \mathbf{Q}_1 & 0 \\ 0 & \mathbf{Q}_2 \end{bmatrix} \begin{Bmatrix} \mathbf{z}_1^{t} \\ \mathbf{z}_2^{t} \end{Bmatrix} + \begin{bmatrix} 0 & \mathbf{R}_1\mathbf{U}_1^{s,k-1} \\ \mathbf{R}_2\mathbf{U}_2^{s,k-1} & 0 \end{bmatrix} \begin{Bmatrix} \mathbf{z}_1^{t+h,k-1} \\ \mathbf{z}_2^{t+h,k-1} \end{Bmatrix} = 0 \tag{12.16}$$

or in a shorter form

$$\mathbf{P}^{it}\mathbf{z}^{t+h,k} + \mathbf{Q}^{it}\mathbf{z}^{t} + \mathbf{R}\mathbf{U}^{it}\mathbf{z}^{t+h,k-1} = 0 \tag{12.17}$$

Since every estimation is based only on the initial conditions of the step $\mathbf{z}^t$, the state variables estimation for the kth iteration are be expressed as:

$$\mathbf{z}^{t+h,k} = \mathbf{A}^{CS,k}\mathbf{z}^{t} \tag{12.18}$$

which yields, with Eq. 12.17,

$$\mathbf{A}^{CS,k} = -\left(\mathbf{P}^{it}\right)^{-1}\left(\mathbf{Q}^{it} + \mathbf{R}\mathbf{U}^{it}\mathbf{A}^{CS,k-1}\right) \tag{12.19}$$

with $\mathbf{A}^{CS,0}$ computed using Eq. 12.12.

12.3 Results

The definition of the amplification matrix of co-simulation schemes provides crucial information about the efficiency of the scheme. Indeed, the spectral radius $\rho(\mathbf{A})$ [7], an indicator of the stability of the scheme, can be deduced from the amplification matrix $\mathbf{A}$. The stability criterion of a numerical scheme is

$$\rho(\mathbf{A}) = \max\left(|\lambda(\mathbf{A})|\right) < 1 \tag{12.20}$$

with λ the function computing the eigenvalues of a matrix. However, a stable scheme does not mean that the scheme is accurate. Indeed, more than the stability, the spectral radius ρ provides a global idea on the transformation that the scheme applied on the real results:

– if $\rho = 1$, the numerical scheme is strictly stable which means that there is at least one mode that conserves its energy;
– if $\rho < 1$, the numerical scheme dissipates energy. That characteristic is a synonym of stability;
– if $\rho > 1$ the numerical scheme introduces energy into the integrated system. This causes instability and the higher the spectral radius, the faster the integrated system will diverge from the analytical solution.

In Fig. 12.3, the spectral radii of 5 different schemes are studied, for Gauß-Seidel and Jacobi coupling schemes applied with forward and backward Euler methods.

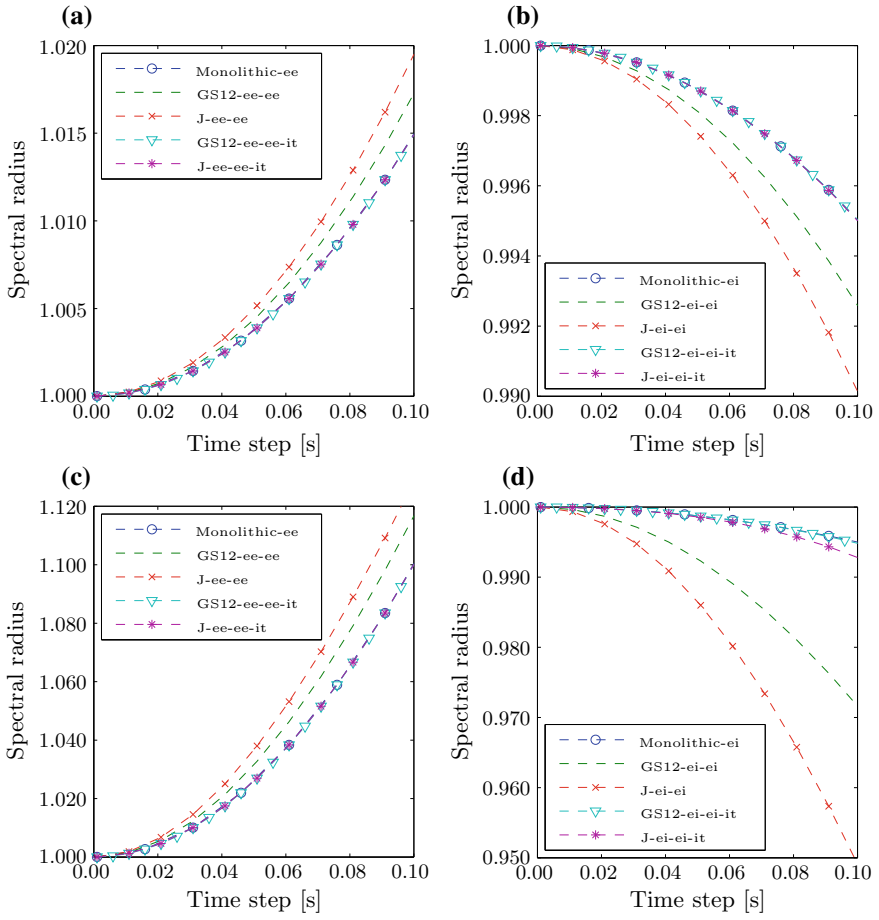

Fig. 12.3 Spectral radii of Gauß-Seidel with the order subsystem 1 before subsystem 2 (GS12) and Jacobi (J) schemes with forward Euler (ee) and backward Euler (ei) integration schemes. (3a) and (3b) are computed for $\frac{k_c}{k_1} = 1$, (3c) and (3d) are computed for $\frac{k_c}{k_1} = 10$ while $\frac{k_2}{k_1} = 1$, $\frac{m_2}{m_1} = 1$ and $d_c = 0$

The latter were chosen for their lack of efficiency in order to illustrate clearly the characteristics of the schemes. In each graph, the reference is assumed to be the monolithic corresponding scheme. A few remarks can be deduced:

- For forward Euler, Figs. 12.3a, c show that the Jacobi scheme is slightly more unstable than the Gauß-Seidel one. Indeed, since Gauß-Seidel is sequential, the second integration input parameters are already a better estimation than in the Jacobi scheme. However, the monolithic scheme provides better results than both coupling schemes.
- For backward Euler, Figs. 12.3b, d show that the Jacobi scheme is slightly more damped than the Gauß-Seidel one which is also more damped than the monolithic scheme. The reason is identical as above.
- Between Figs 12.3a–d, the coupling stiffness ratio $\frac{k_c}{k_1}$ was multiplied by 10. It can be noticed that the stiffer the coupling, the less accurate the results are.
- In each graph, a 1-iteration version of both schemes is studied using Eq. 12.19. Generally, the results are better than each non-iterated corresponding scheme. It can also be proven that, for explicit Euler schemes, it converges to the corresponding monolithic scheme in a single iteration for both Jacobi and Gauß-Seidel coupling methods.

More than the spectral radius, the frequency error and the damping ratios can be computed using the amplification matrix of a scheme. Those parameters are defined using the continuous equivalent λ_i^c of the discretized form of the eigenvalues λ_i of the amplification matrix $\mathbf{A}$ given in Eq. 12.21:

$$\lambda_i^c = \frac{\ln \lambda_i}{h} = \sigma_i \pm j\omega_i \tag{12.21}$$

with h the timestep. From this definition, the damping ratio ξ_{ω_i} and the frequency error ϵ_{ω_i} of mode i can be computed using Eqs. 12.22a and 12.22b:

$$\xi_{\omega_i} = \frac{-\sigma_i}{\sqrt{\sigma_i^2 + \omega_i^2}} \tag{12.22a}$$

$$\epsilon_{\omega_i} = \frac{\sqrt{\sigma_i^2 + \omega_i^2} - \omega_{0i}}{\omega_{0i}} \tag{12.22b}$$

with ω_{0i} the analytical eigenfrequency of mode i. Figure 12.4 illustrates these parameters for mixed forward/backward Euler schemes taking into account that backward Euler is always applied on the second subsystem. Since Gauß-Seidel seemed to provide the best performance, the situations in which both subsystems are integrated using forward and backward Euler methods, with Gauß-Seidel coupling, are taken as references to compare the mixed schemes with. It can be observed that:

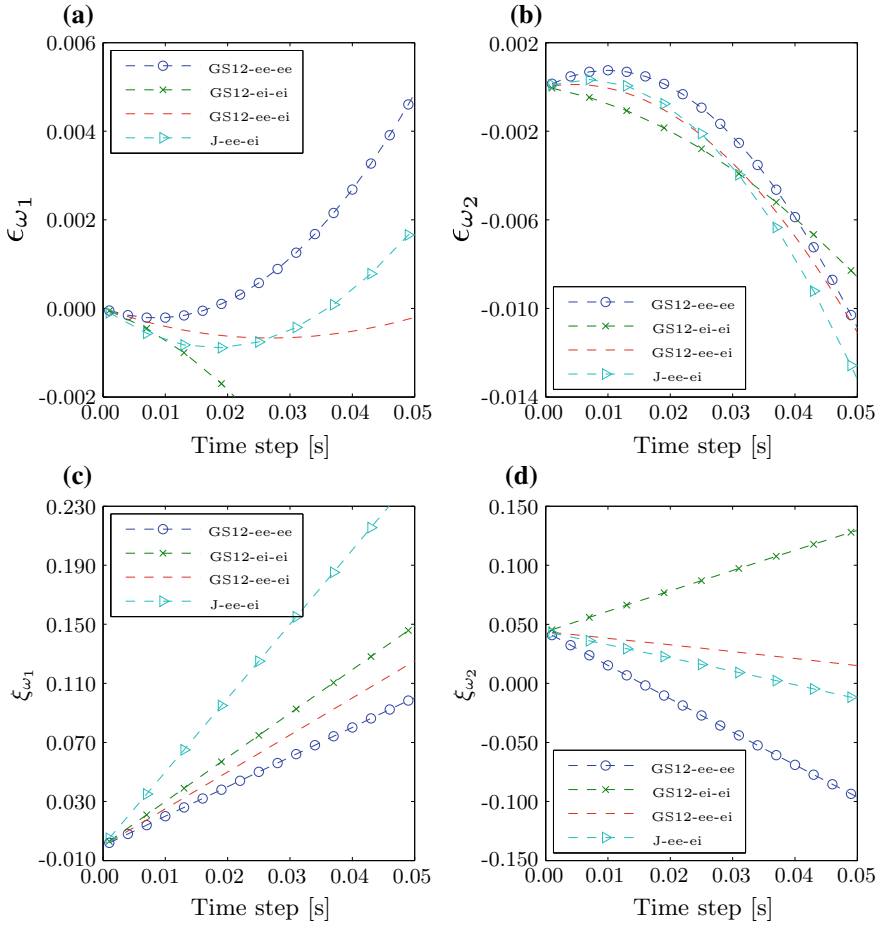

Fig. 12.4 Relative frequency error (ϵ_{ω_i}) and damping ratio (ξ_{ω_i}) of Gauß-Seidel with the order subsystem 1 before subsystem 2 (GS12) and Jacobi (J) schemes with mixed forward Euler (ee) and backward Euler (ei) integration schemes. (4a) and (4c) concern the first eigenfrequency ω_1 and (4b) and (4d) concern the second eigenfrequency ω_2 with $\omega_1 < \omega_2$ while $\frac{k_c}{k_1} = 10$, $\frac{k_2}{k_1} = 1$, $\frac{m_2}{m_1} = 1$ and $d_c = 0.2$

- for small time steps, the frequency error of the second eigenfrequency is smaller in mixed schemes than in fully explicit/implicit schemes. However, the fully explicit scheme seems to provide a smaller frequency error for the first eigenfrequency;
- both mixed schemes provide a damping closer to 0 for the second eigenfrequency. However, for the first eigenfrequency, the fully explicit scheme provides, once again, a smaller damping;
- both frequency errors converge to 0 with the time step;
- both damping coefficients converge to the physical damping coefficient which means that the numerical damping converges to 0.

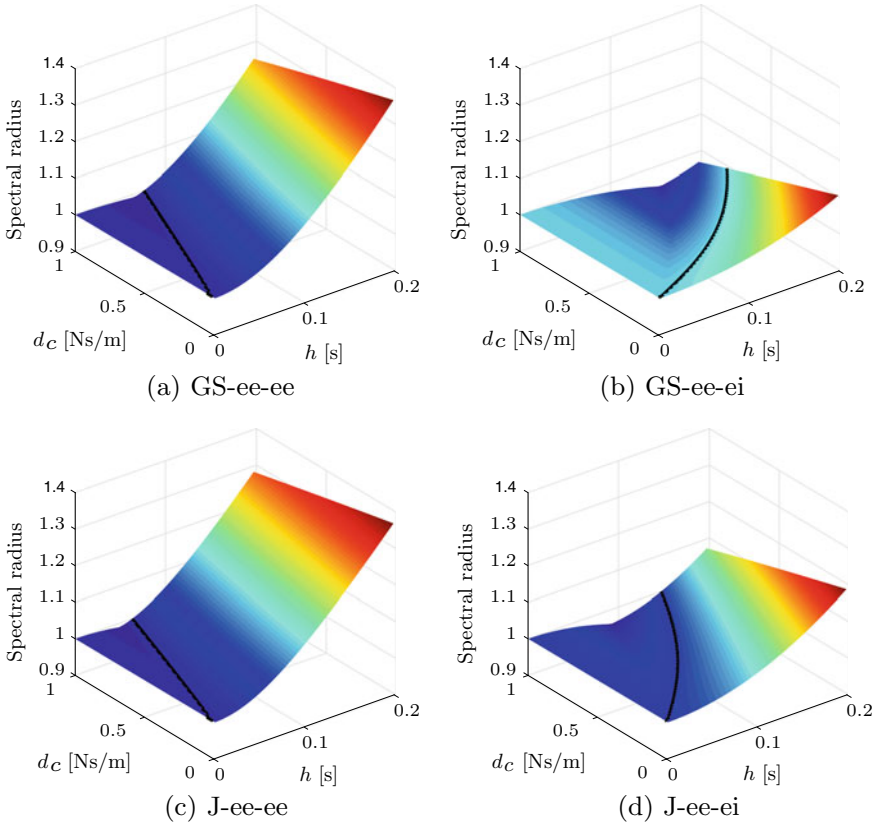

Fig. 12.5 Gauß-Seidel (a, b) and Jacobi (c, d) schemes applied with different integration schemes with $\frac{m_2}{m_1} = 1$, $\frac{k_2}{k_1} = 1$ and $\frac{k_c}{k_1} = 10$. **a** and **c** represents forward Euler (ee) for both subsystems and **b** and **d** represents forward Euler (ee) for subsystem 1 and backward Euler (ei) for subsystem 2. The stability and instability regions are separated by a line at which the spectral radius is 1

Figure 12.5 shows the impact of the link damping d_c on the stability of mixed Jacobi and Gauß-Seidel schemes through their spectral radii. It turns out that:

- both mixed schemes provide spectral radii closer to 1 than the corresponding fully explicit scheme;
- once again, the Gauß-Seidel scheme appears to be better than the Jacobi scheme;
- both mixed scheme offer a larger stability region that grows with the link damping d_c. However, the price for this larger stability region is a larger damping of the solution for a same time step.

12.4 Conclusions

Such as for classic monolithic mathematical representation of mechanical system, the amplification matrix of co-simulated schemes can be written and interesting properties (such as the spectral radius, the frequency error and the damping ratio) can be deduced:

- each coupling scheme used exhibits a zero-stable behavior;
- co-simulation schemes are less accurate than the corresponding monolithic method;
- the Jacobi scheme usually provides a reduced accuracy in comparison with the Gauß-Seidel scheme. This phenomenon is explained by their respective parallel and sequential behavior [5];
- the results provided by iterated schemes are usually better than the corresponding non-iterated schemes. Once again, the sequential Gauß-Seidel scheme appears to give the best results;
- mixed integration schemes produce larger stability regions for the time step choice. However, in return, the damping induced by those methods is larger for a same time step.

References

1. Fernández Ruiz, J., Alves Costa, P., Calada, R., Medina Rodríguez, L.E., Colao, A.: Study of ground vibrations induced by railway traffic in a 3D FEM model formulated in the time domain: experimental validation. Struct. Infrastruct. Eng. **13**, 652–664 (2017)
2. Gardien, W., Stuit, H.G.: Modelling of soil vibrations from railway tunnels. J. Sound Vib. **267**, 605–619 (2003)
3. Olivier, B., Connolly, D.P., Alves Costa, P., Kouroussis, G.: The effect of embankment on high speed rail ground vibrations. Int. J. Rail Transp. **4**, 229–246 (2016)
4. Kouroussis, G., Verlinden, O.: Prediction of railway ground vibrations: accuracy of a coupled lumped mass model for representing the track/soil interaction. Soil Dyn. Earthq. Eng. **69**, 220–226 (2015)
5. Busch, M.: Zur effizienten Kopplung von Simulationsprogrammen. Ph.D. Thesis, Kassel University Press (2012)
6. Géradin, M., Rixen, D.: Mechanical Vibrations: Theory and Application to Structural Dynamics. Wiley (2015)
7. Hairer, E., Wanner, G.: Solving Ordinary Differential Equations. Springer, Berlin (1993)